

An Optical Search for Small-Size Debris in GEO and GTO

T. Schildknecht⁽¹⁾, R. Musci⁽¹⁾, M. Ploner⁽¹⁾, W. Flury⁽²⁾, J. Kuusela⁽³⁾, J. de Leon Cruz⁽⁴⁾,
L. de Fatima Dominguez Palmero⁽⁴⁾

⁽¹⁾ *Astronomical Institute, University of Bern, Sidlerstrasse 5, CH-3012 Bern, Switzerland*
Email: thomas.schildknecht@aiub.unibe.ch
Email: reto.musci@aiub.unibe.ch
Email: martin.ploner@aiub.unibe.ch

⁽²⁾ *ESA ESOC, Robert-Bosch-Strasse 5, 64293 Darmstadt, Germany*
Email: Walter.Flury@esa.int

⁽³⁾ *ASRO, Turku, Finland*
Email: jyri.kuusela@asro-space.com

⁽⁴⁾ *Instituto de Astrofísica de Canarias, 38200 La Laguna, Tenerife, España*
Email: jmlc@ot.iac.es
Email: ldp@ll.iac.es

ABSTRACT

The space debris population in low Earth orbits (LEO) has been extensively studied during the last decade and reasonable models covering all size ranges were produced. Information on the distribution of objects in high-altitude orbits, however, is still comparatively sparse.

Optical telescopes are the sensors of choice to observe objects in high-altitude Earth orbits. The European Space Agency (ESA) was thus setting up an optical debris survey system using its 1-meter telescope on Tenerife, Canary Islands. This system is operational since 1999 and is used primarily for surveys of the geostationary ring (GEO) and the geostationary transfer orbit (GTO) region. The results from the last three years of observations changed our understanding of the space debris population in GEO considerably: A hitherto unknown, but significant, population of small-size objects with diameters as small as 10 centimeters has been detected. Moreover, distinct debris clouds – presumably stemming from individual explosions – were identified.

Small-size debris are also expected in GTO orbits where a number of explosive events, associated with spent upper stages, were observed. First results from a survey of eccentric orbits, covering in particular the GTO region used by the European Ariane launchers, indicate that there is small-size debris not only in the GTO orbit range, but also in a much wider range of orbits.

1. INTRODUCTION

Since the launch of Syncom-2 in 1963 about 950 satellites or rocket upper stages have been placed into the geostationary ring (GEO) or into its vicinity. Routine space surveillance of GEO with ground-based radars and optical telescopes of the United States' Space Surveillance Network (SSN) is able to detect objects of approximately 1-meter minimum size. Smaller objects, however, must exist since two explosions are known to have occurred in GEO (a breakup of an Ekran spacecraft in 1978 and an explosion of a Titan rocket upper stage in 1992).

ESA has been recognizing the paramount importance of protecting the geostationary ring from contaminating space debris since a long time. It was evident that the search for fragments in the geostationary ring and a better knowledge of the debris population in GEO are prerequisites in order to understand the future evolution of the debris population, to assess the collision risk and to define suitable and cost-efficient mitigation measures. Consequently ESA around 1990 initiated a program to establish optical debris searches in GEO and high-altitude regions.

A first step consisted in the optical and mechanical upgrade of a Zeiss 1-meter telescope to make it suitable for debris observations. At the same time a large cryogenically cooled CCD camera consisting of a 4k x 4k pixel CCD mosaic was procured. The ESA Space Debris Telescope is installed in the Optical Ground Station (OGS) at Observatory of the Teide in Tenerife, Canary Islands. Optical survey for small sized debris in GEO eventually started in summer 1999.

The first results from these surveys showed a considerable population of small-sized objects with sizes as small as 10 centimeters. Furthermore some clusters of objects were identified in the orbital element space. Objects in these clusters have similar dynamical characteristics and therefore the only reasonable explanation for the origin of these clusters are explosions.

In the course of the GEO surveys many objects on apparently ‘peculiar’ orbits were found. Assuming circular orbits these objects seemed to be at altitudes from 50’000 to 70’000 kilometers. We suspected a ‘contamination’ of the GEO samples by objects on highly elliptical orbits. This hypothesis could only be proved by following-up a subset of the objects in order to acquire reasonably well-determined elliptical orbits.

It was also evident that the GEO data contained some objects on geostationary transfer (GTO) orbits which were detected when they were near the apogee. In contrary to the GEO region many explosions were documented in GTO orbits. Some upper stages and motors in GTO are notorious for explosions! ESA is especially interested in the fate of debris generated by the explosion of Ariane third stages. Breakups of these rocket bodies were observed sometimes decades after their insertion into orbit. Ariane third stage passivation employed on all Ariane missions since October 1993 successfully prevented explosions of any Ariane third stage launched after this date. The US-STRATCOM catalogue contains debris objects in GTO which are smaller than the smallest catalogued objects in GEO. However, for GTO objects the catalogue is expected to be incomplete for object sizes substantially smaller than the limit of the catalogue of about 40 centimeters.

This paper describes the ESA GEO and GTO surveys and presents results from recent observation campaigns. We will particularly focus on the results for objects on elliptical orbits.

2. SURVEY TECHNIQUES

A so-called ‘sky survey’ is monitoring the sky for temporal changes, i.e. for objects which have changed their brightness or their position. In the case of a survey for GEO or GTO objects we are looking for objects which move with respect to the stellar background. This can be done either by searching for elongated images on a single, siderally tracked frame or by searching for objects which changed their position on frames taken at different epochs. We use the latter approach for which we developed the so-called masking technique [1]. If an object with a reasonable apparent motion is found on a series of frames its position in a celestial reference frame is determined on each exposure by means of reference stars. By ‘reasonable’ we mean within the range of expected apparent motion for GEO and GTO objects. Using these positions an initial orbit is determined and the orbital elements and the positions are correlated with a catalogue of known GEO objects. In most cases the discoveries consist of a set of two to three observations spaced by one to two minutes only. The extremely short arc of the detection observations does not allow for a full 6-parameter orbit determination and we are therefore forced to assume circular orbits.

2.1. GEO Surveys

Debris released from objects in GEO, e.g. mission related objects or material released due to aging processes, is expected to stay in orbits similar to the orbits of their parent bodies. Even pieces stemming from explosions in GEO will generally remain in the GEO region. The energy increment or decrement they get during the explosion is usually not sufficient to considerably alter their orbital plane or their semimajor axis. The debris will not only start with orbits similar to their parent objects, but their orbits will also undergo similar perturbations and thus evolve in a similar way (the latter may not be true for objects with a very large area to mass ratio which react differently to radiation pressure forces). It is therefore reasonable to assume the simple hypothesis that the catalogued GEO objects trace the debris population. It is obvious that the detailed orbital characteristics of these two populations will certainly differ from each other (we expect debris from distinct explosion events) but in general we expect them to occupy the same region in the orbital element space.

Figure 1 shows the apparent density of the catalogued GEO objects (gray shaded area) in the right ascension-declination-space as seen from the geocenter. The sinusoidal pattern is due to a specific distribution of the orbital planes, which in turn is due to gravitational perturbations. The orbital planes of uncontrolled objects in GEO exhibit precessional motions, which manifest themselves in periodic variations of the inclinations between 0 and 15 degrees with a period of about 53 years. These precessional motions also result in a correlation between the inclinations and the right ascensions of the ascending nodes.

When defining the search fields there is a series of observational constraints to be taken into account. First of all the objects should be observed under good illumination conditions (the so-called phase angle should be small), which means that the best locations are near the Earth shadow cone (but still outside the shadow region!). Dense stellar background regions, in particular the Milky Way, must be avoided. The fields should be at high elevations for a good part of the night; the angular distance from the moon should be maximized, etc. Last but not least the field should cover the dense region of the catalogue population where we expect – according to the mentioned hypothesis – the most debris pieces. The fields of the ESA 2001 spring campaign shown in Figure 1 satisfy these criteria.

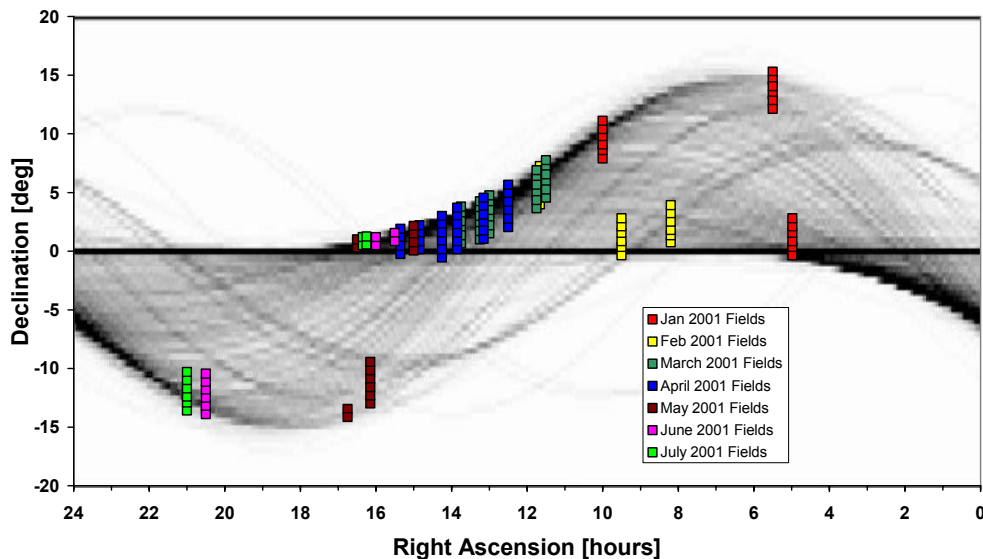


Figure 1: Survey fields of the spring 2001 campaign (small squares) in the right ascension-declination space as seen from the geocenter. The gray-shaded background indicates the apparent density of the catalogued GEO objects.

2.2. GTO Surveys

Searching for objects in GTO is much more demanding than in GEO. In contrary to GEO the apparent positions of objects in GTO are not restricted to a 30-degree wide region centered on the equator. Moreover the apparent angular velocity of GTO objects varies over a wide range from a few arcseconds per second to many arcminutes per second. In order to implement an efficient detection strategy we look for regions where the changes in apparent velocity are small so that we may optimize the tracking and the integration time. This is the case near the apogees. In the regions around the apogees the objects also move slowest and thus stay there for most of the time. There is a disadvantage of searching objects near the apogees of their orbits: the distances are largest in these regions, and thus the apparent magnitudes are faintest. It can, however, be shown that the advantage of the small changes in apparent angular velocity outperforms the disadvantage of large distances.

Figure 2 shows typical examples of apparent passes of GTO objects as seen by an observer in the horizon system. Two cases of mean motion n and two cases of perigee location ω were chosen for this illustration. The apparent motion of an object is indicated by arrows for the $n=2.16$ rev/day, $\omega=270^\circ$ case. The examples are such that the objects reach their apogees at the time when they also pass the meridian (azimuth = 180°). Near the apogee (between the markers 2 and 3) the objects move mostly parallel to the GEO ring (negligible velocity in declination) from east to west. Between the points 2 and 3 the objects are drifting – depending on the actual orbit – for about 3 to 5 hours with an almost constant velocity of 7 to 11 arcseconds per second in right ascension.

The fact that the apparent motions of GTO objects near their apogees are constant over a considerable time period allows for a simple survey scheme. We decided to use an adapted version of the GEO technique, where essentially only the tracking speed during the exposure was modified. The tracking rate in right ascension during the exposure is set to either 7.5 or 10.5 arcseconds per second instead of 0 arcseconds per second for the GEO surveys (for more details see [2]).

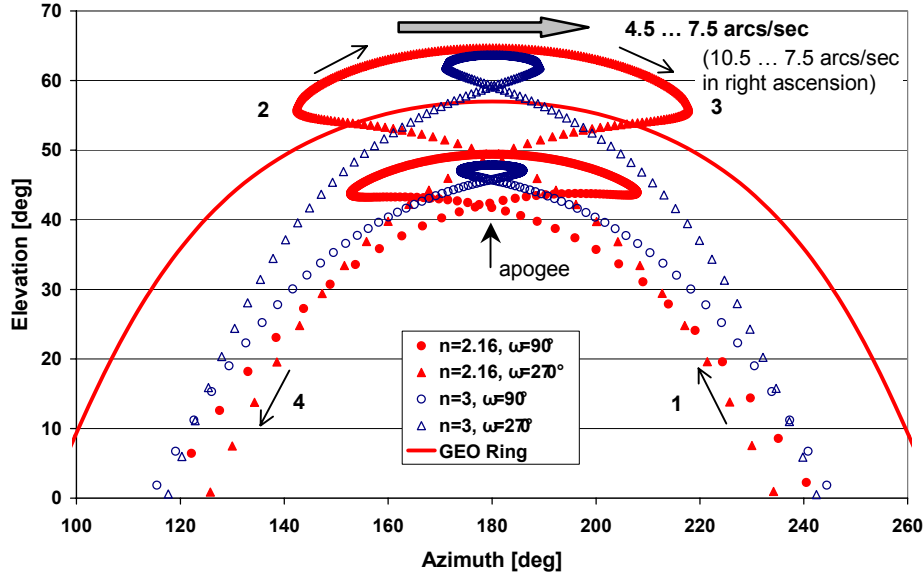


Figure 2: Apparent passes of GTO objects as seen by an observer in the horizon system. Apogee passages in the meridian for two cases of mean motion n and two cases of perigee location ω . The solid line indicates the GEO ring.

3. ESA SURVEYS

3.1. Results from GEO surveys

ESA has been conducting several GEO survey campaigns during the past years. Table 1 gives an overview of the ESA GEO campaigns until April 2003. The table includes the 1999 test campaign, which consisted in fact of a first, very limited series of system tests. The terms ‘correlated’ and ‘uncorrelated’ refer to objects/detections which correlate or do not correlate with the catalogue. We used the unclassified part of the USSTRATCOM catalogue as our reference. By ‘detection’ we denote the detection of an object within a single 30-minute observation series. Some of these detections may actually refer to the same object, i.e. we may have incidentally re-observed some of the objects during the campaign. We subsume all detections that seem to belong to the same real object under the term ‘correlated object’ (if the object is part of the catalogue) or ‘uncorrelated object’ (if the object is not part of the catalogue) respectively mutually correlating all detections of a campaign. This latter task is identical with the creation and maintenance of a temporary catalogue of orbital elements for the unknown objects and has been performed for the first campaign only. During the 2002 and the 2003 campaigns part of the surveys were optimized for the detection of GTOs (see Section 3.2).

Table 1. ESA GEO Campaigns

	Aug/Sept 1999 (1 st IADC Campaign)	Jan – Jul 2001	Jan – Dec 2002 (2 nd IADC Campaign)	Jan – Apr 2003
Obs. Time	13 nights / 49 h	82 nights / 521 h	90 nights / 613 h	25 nights / 154 h
Optimized for GEO	49 h	521 h	413 h	77 h
Optimized for GTO	-	-	200 h	77 h
Scanned Area	895 deg ²	11'200 deg ²	12'300 deg ²	3'500 deg ²
Frames	5'400	62'500	80'600	13'200
Image Data	52 GB	500 GB	670 GB	105 GB
Correlated detections	180	2'023	1960	523
Correlated objects	56	367	404	219
Uncorrelated detections	348	1'587	2389	457
Uncorrelated objects	150	?	?	?

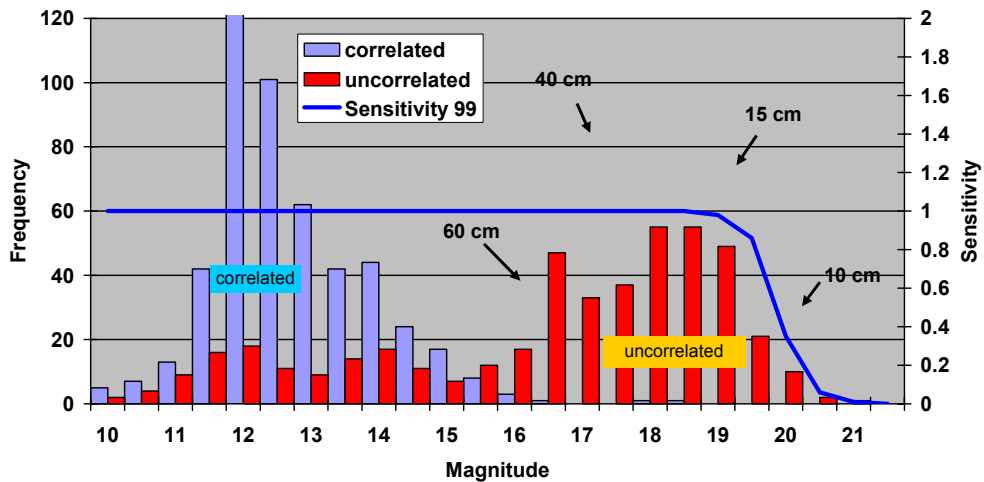


Figure 4: Absolute magnitude distribution for the detections of the January to April 2003 campaign.

At this point it is very important to draw our attention again to the fact that all surveys in Table 1 suffer from observational biases. Or in other words ‘what we see depends on where and when we look’. The numbers given in Table 1 could therefore be misleading, e.g. when simply taking the ratio of uncorrelated to correlated detections as a measure to estimate the total number of debris objects!

Absolute Magnitude Distribution

Figure 3 shows the absolute magnitude distribution of all detections from 2002 campaigns. The corresponding figure for the data set of the January to April 2003 campaign is given in Figure 4. The solid lines indicate the system sensitivity as determined from independent calibration measurements. All magnitudes have been reduced from apparent magnitudes to so-called absolute magnitudes by correcting for the illumination phase angle. For the scattering properties we assumed a simple Lambertian sphere. No reduction to a common distance has been done because of the uncertainties of the determined orbits (see below). The value of this correction would be less than 0.5 magnitudes in most cases. The magnitudes are astronomical ‘V magnitudes’ and have an accuracy of a few 0.1 magnitudes except for the very faint objects where errors could amount to 0.5 – 1 magnitude. The indicated object sizes were derived by assuming Lambertian spheres and a Bond albedo of 0.1. Both assumptions, however, are uncertain, as long as we don’t know the nature of the observed objects.

The distribution is bimodal for both campaigns. The distribution of the correlated detections has its peak at about magnitude 12.5 and spreads from about magnitude 10 to 15. It is also slightly asymmetric with the slope on

the fainter end being shallower. This distribution nicely reflects the size distribution in the catalogue. The uncorrelated objects seem to be concentrated in a broad strong peak around magnitude 18 to 18.5 and in a second much less pronounced peak which follows more or less the distribution of correlated objects.

The bright objects in the latter peak are most likely all ‘known’, large objects, which did not correlate with the catalogue for several reasons. Some of these objects are classified and were therefore not included in the ‘unclassified’ version of the catalogue. Others might well be in the catalogue but did not correlate due to insufficient accuracy of the catalogue. In many cases these objects are members of groups of satellites co-located in the same 0.1-degree longitude slot. They often correlate with several objects in the catalogue, again due to the limited accuracy of the catalogue, and thus end up as ‘uncorrelated’ due to confusion. Finally the catalogue might be incomplete at the fainter end.

The uncorrelated objects in the range from magnitude 15 to 21 are smaller than the minimum size of the objects in the catalogue. The apparent main peak of this population at about magnitude 18 is in fact not a peak, because the cutoff in number of objects fainter than about magnitude 19 is entirely due to the sensitivity limit of the observation system (see the line indicating system sensitivity). The real luminosity function beyond magnitude 19 could therefore still increase!

The data from the 2003 campaign nicely confirms the results from the 2002 survey.

Inclination Distribution

The inclination distributions for the January to December 2002 and the January to April 2003 campaigns are shown in Figure 5 and Figure 6, respectively. The distribution of the uncorrelated detections for the year 2002 (Figure 5) roughly follows the distribution of the correlated detections for inclinations lower than about 11 degrees. For higher inclinations there is a clear excess of uncorrelated detections. The January to April 2003 campaign (Figure 6) contains much less observations and therefore the distribution is more affected by observational selection biases. Nevertheless the excess of uncorrelated detections at inclinations higher than about 12 degrees is clearly visible.

Distribution of Semimajor Axes

Figure 7 shows the distributions of the so-called ‘inferred’ semimajor axes of the 2002 campaign. By the term ‘inferred’ we denote that these semimajor axes are in fact the radii of the circular orbits determined from the detection observations (the extremely short arc of the detection observations does not allow for a full 6-parameter orbit determination). The corresponding distribution of the 2003 campaign is very similar and therefore not shown. Both, the correlated and the uncorrelated objects, are concentrated around the nominal GEO altitude. The semimajor axes of the uncorrelated objects, however, are much more dispersed showing a significant asymmetry with an excess at large values.

It is important to keep in mind that inferred semimajor axes are in fact determined assuming circular orbits, which is certainly not the case for all objects. In general, fixing the eccentricity at a wrong value may result in a large error of the inferred semimajor axis. Part of the spread for the uncorrelated objects, as well as some of the large values may be due to this effect. Objects on highly eccentric orbits having their apogee near GEO may mimic objects in much higher circular orbits when observed at apogee.

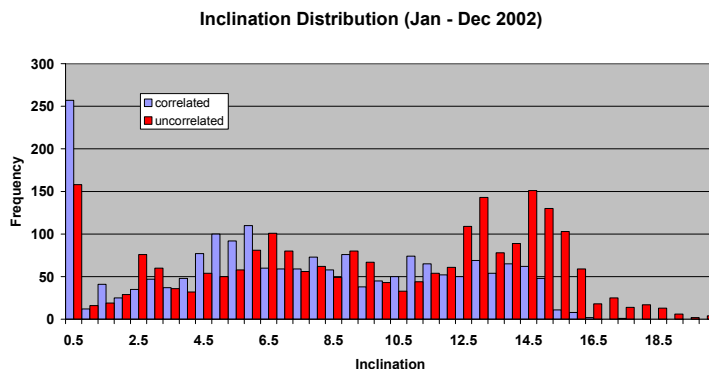


Figure 5: Inclination distribution for detections of the January to December 2002 campaign (inclination in degrees).

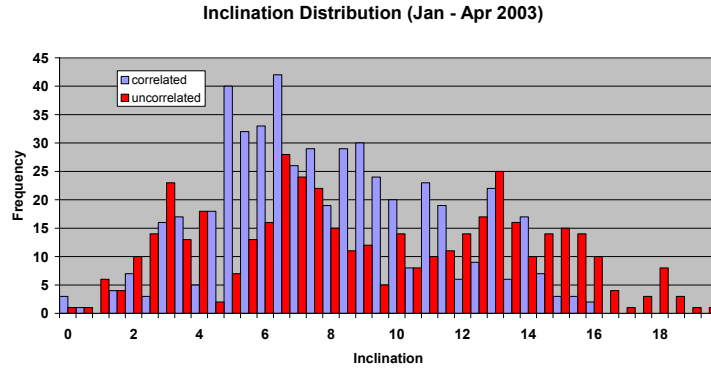


Figure 6: Inclination distribution for detections of the January to April 2003 campaign (inclination in degrees).

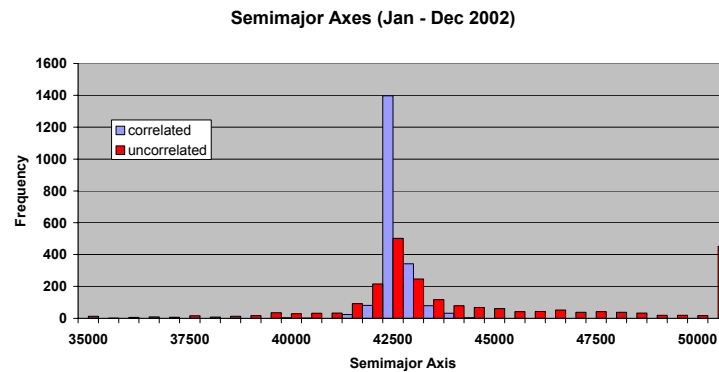


Figure 7: Distribution of semimajor axes for detections of the January to December 2002 campaign (semimajor axis in kilometers).

Orbit Inclination and Right Ascension of Ascending Node

The inclinations i and the right ascensions of the ascending nodes Ω are strongly correlated for the TLE population as we have seen in Section 2.1. Figure 8 and Figure 9 give both elements for all correlated and uncorrelated detections of the 2002 and the 2003 campaign respectively. The distinct figure outlined by the correlated objects is due to the explained 53-year precession period of the orbital planes. Assuming that the objects started with orbits of 0 degree inclination the position in the diagram is indicating the time since the end of active inclination control. The orbits gradually evolve from low inclination and at right ascension of the ascending node of about 100 degrees to higher inclinations and lower right ascension of the node until they reach the maximum inclination of 15 degrees after 26.5 years. The oldest catalogue objects have already passed this point.

The bulk of the uncorrelated objects lie again on the mentioned evolution track but with a much larger spread. In addition there is a ‘background’ component with a more homogeneous distribution in the (Ω, i) -space especially noticeable in the right diagram of Figure 8. The most striking features, however, are the distinct clusters of objects. Prominent concentrations are found in Figure 8 at $\Omega \approx 20^\circ / i \approx 13^\circ$, $\Omega \approx 15^\circ / i \approx 14.5^\circ$, $\Omega \approx 10^\circ / i \approx 15^\circ$ (all with an elliptical shape), and at $\Omega \approx 50^\circ / i \approx 8^\circ$ and $\Omega \approx -12^\circ / i \approx 12.5^\circ$ (both ‘banana-shaped’). There are much less observations from the 2003 campaign compared to the 2002 campaign but some concentrations seen in Figure 8 may be found in Figure 9 as well.

We have checked some of the clusters for multiple sightings of the same objects and conclude that they are real (a pure selection effect can be excluded). The only reasonable explanation for the origin of these clusters are explosive events.

The explanation for the ‘background’ component is more difficult. At this time we cannot decide if this component is real or an artifact due to the assumed circular orbits. As explained in the paragraph on the inclination distribution, objects on highly elliptic orbits like GTOs may affect the results and could at least partly be responsible for the ‘background’ component.

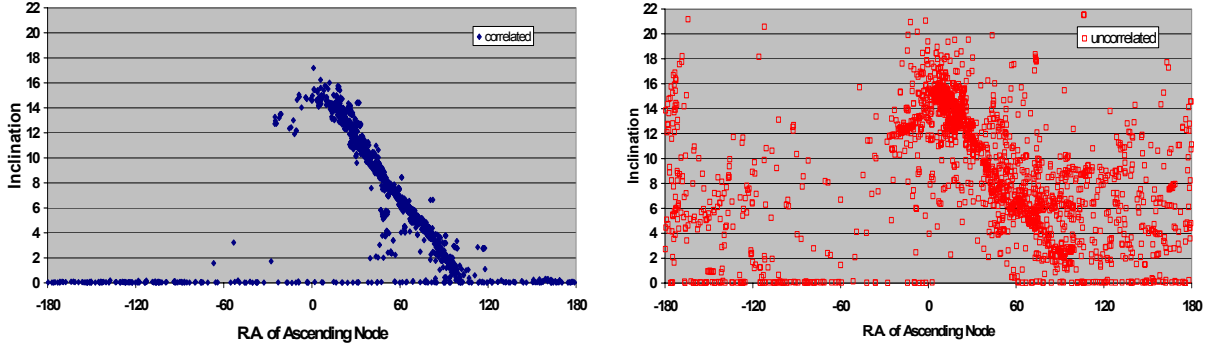


Figure 8: Inclination as a function of the right ascension of the ascending node for the correlated (left) and uncorrelated (right) detections of the January to December 2002 campaign.

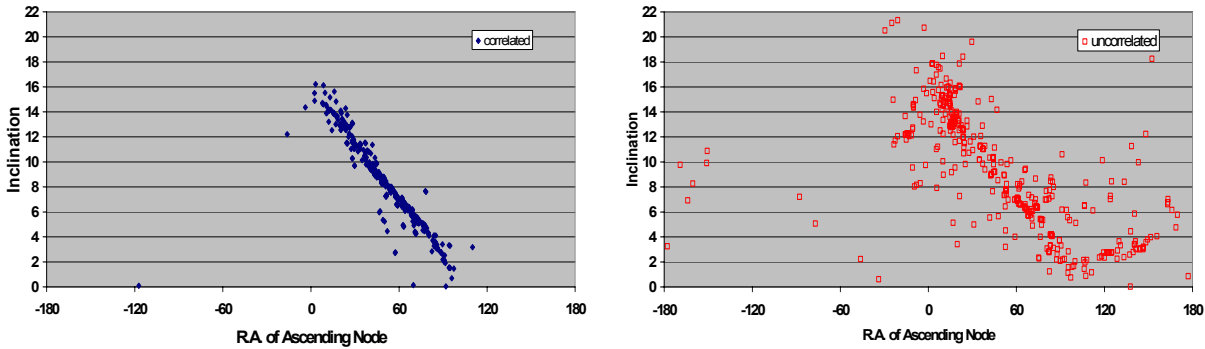


Figure 9: Inclination as a function of the right ascension of ascending node for the correlated (left) and uncorrelated (right) detections of the January to April 2003 campaign.

3.2. Results from GTO surveys

One restriction of the results shown above is that circular orbits had to be inferred. This is certainly a good approximation for GEO objects. But for objects with highly eccentric orbits we have to expect that the orbital elements of the inferred circular orbits are considerably different from the real orbital elements. The ‘contamination’ by elliptical orbits will in particular affect the distribution of semimajor axes and the orientation of the orbital planes, i.e. the inclination versus right ascension of the ascending node (Ω , i) distribution.

During a GEO survey objects with high eccentricities are normally detected when they are near the apogee. By inferring circular orbits for these objects we in fact interpret the change in the true anomaly near the apogee as the mean motion of a circular orbit. The velocity of an object in an elliptical orbit at the apogee is slower than the corresponding velocity of an object on a circular orbit with a radius equal to the apogee radius of the former. This in turn means that the radius of the inferred circular orbit is larger than the apogee radius of the elliptical orbit. For an object observed at apogee in a geocentric system the semimajor axis a_{circ} of the inferred circular orbit is given by

$$a_{\text{circ}} = a \left(\frac{1+e}{1-e} \right)^{2/3},$$

where a and e are the real semimajor axis and eccentricity. For a GTO object with $a = 24'500$ km and $e = 0.7$, i.e. apogee at the GEO ring, a radius of $a_{\text{circ}} \sim 78'000$ km would result. If we take the parallax for the Tenerife site into account we get $a_{\text{circ}} \sim 63'600$ km.

The lack of information about the eccentricity will obviously cause errors in the estimation of the remaining orbital elements. For objects with considerably eccentric orbits like GTOs the errors of the inferred orbital elements may be so large that the results for these objects mimic a dynamically totally different population compared to the real one. We therefore decided to perform real-time follow-up observations of a subset of the objects shortly after discovery. Usually a short series of observations was acquired about 15 to 30 minutes after the first detection. The

combination of these observations with the discovery observations allowed in all cases the determination of a reliable 6-parameter orbit. Needless to say that the follow-up observations significantly reduced the available survey time.

During the campaigns from July 2002 to April 2003 about half of the survey time was devoted to GTO surveys. Technically the only difference between these GTO surveys and our traditional GEO surveys is the telescope tracking during the exposures. While in the GEO case the telescope is tracking with $15''/\text{sec}$ in right ascension (telescope fixed in the horizon system) we track in the GTO case either with $7.5''/\text{sec}$ or $10.5''/\text{sec}$ – the range of expected apparent motion of GTO objects at apogee. During the GTO surveys we tried to follow-up all objects for which the circular orbit determination yielded semimajor axes larger than $47'000$ km. Eventually a reliable 6-parameter orbit could be determined for 109 objects.

Figure 10 gives the magnitude distribution for this data set. The magnitudes were corrected for the phase angle but not yet reduced to a common distance. It is therefore not possible to assign an object size to a given magnitude. The solid line is again indicating the instrument sensitivity. Most of the uncorrelated objects are fainter than magnitude 16 and thus quite small in size.

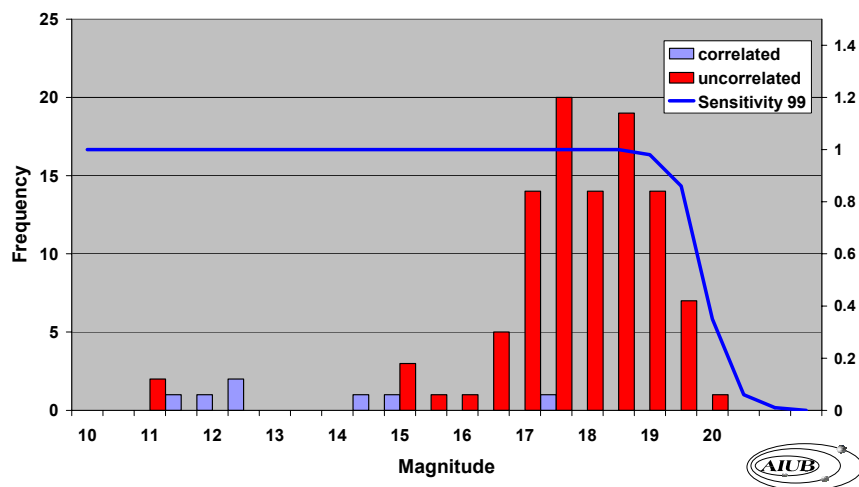


Figure 10: Magnitude distribution for 109 objects with elliptical orbits.

The distribution of the mean motion n for the 101 uncorrelated objects is given in Figure 11. There seem to be two maxima: a broad maximum with a peak at $n=1$ and a second maximum in the range from $n=2.1, \dots, 2.8$. The latter is the typical range for GTO orbits. The corresponding distribution for the objects in the catalogue is given in Figure 11 (right). (The catalogue data was filtered for with $e=\{0.1, 0.9\}$, $i=\{-20.0, 20.0\}$, $n=\{0.3, 6.0\}$.) The first peak at $n=1$ is clearly missing in the catalogue data whereas the GTO region is fairly populated.

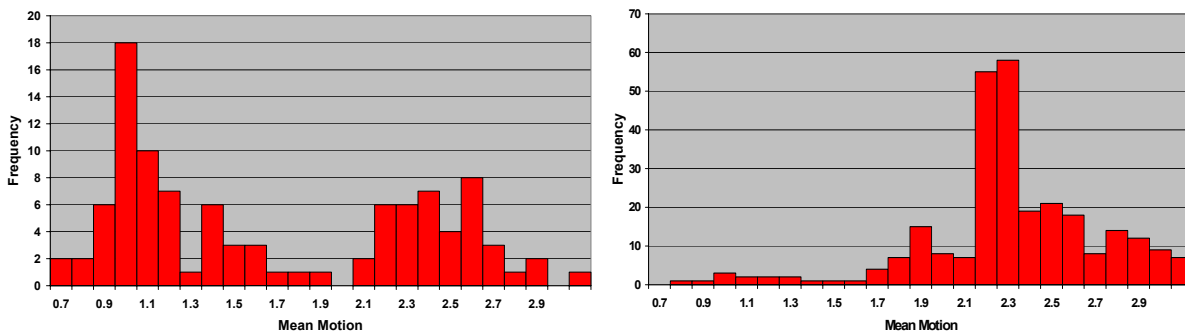


Figure 11: Distribution of the mean motion for 101 uncorrelated objects with elliptical orbits (left) and corresponding distribution of objects in the catalogue (right). (Mean motion in revolutions per day.)

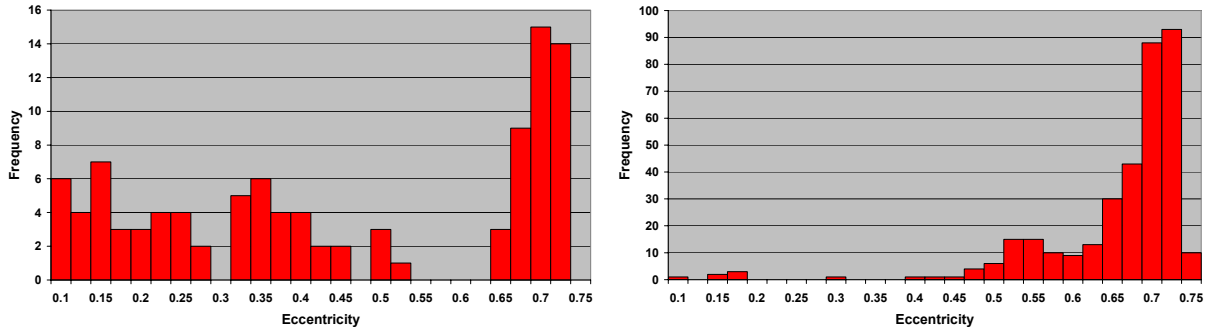


Figure 12: Distribution of eccentricity for 101 uncorrelated objects with elliptical orbits (left) and corresponding distribution of objects in the catalogue (right).

A similar discrepancy between the observed and the catalogue data is found for the distribution of the eccentricity (Figure 12 left and Figure 12 right respectively). More than half of the objects found are in orbits with eccentricities between 0 and 0.5, a region where there are almost no objects in the catalogue. The GTO orbit range from 0.5 to 0.75, on the other hand, is seen in both, the observation data and the catalogue.

Figure 13 and Figure 14 show the eccentricity as a function of the mean motion for the 101 uncorrelated objects and the corresponding catalogue data respectively. The lines indicate locations of constant apparent motion in right ascension when the objects are in the apogee. The solid lines define the boundaries of the region where the GTO surveys were able to detect objects. Objects moving slower than about $5''/\text{sec}$ or faster than $15''/\text{sec}$ would not have passed our detection filter or the subsequent selection criteria to initiate follow-up observations. The region where the surveys were most sensitive lies between the dotted and the dashed lines. Comparing the two figures we note that a) there is a population of small objects in the region of the GTO orbits (near-horizontal branch at upper right), and b) that there is a considerable population of objects with a mean motion near one and eccentricities ranging from 0.05 to 0.5 – a region with almost no corresponding objects in the catalogue. The nature and origin of this second population is currently unknown. Simulations will be required to test if e.g. gravitational resonance effects could increase the eccentricity of GEO objects by such large amounts within a few decades.

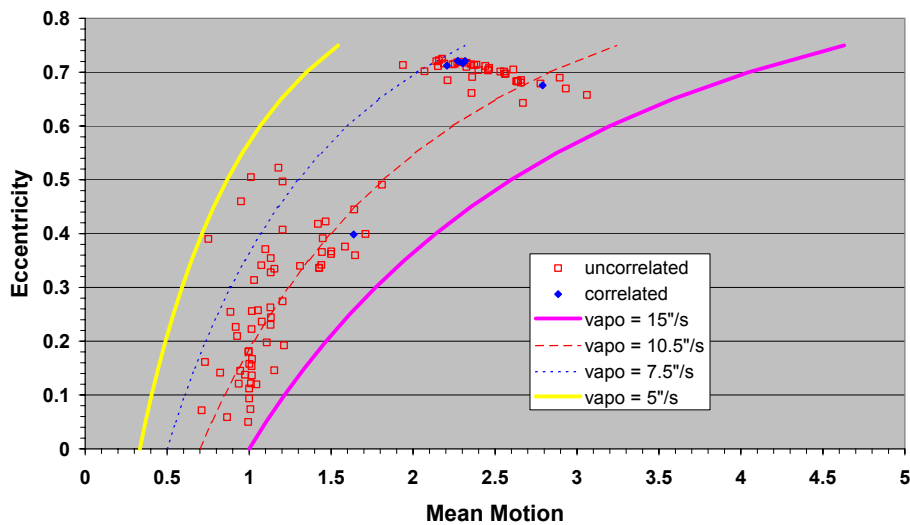


Figure 13: Eccentricity as a function of the mean motion for 101 uncorrelated objects with elliptical orbits.

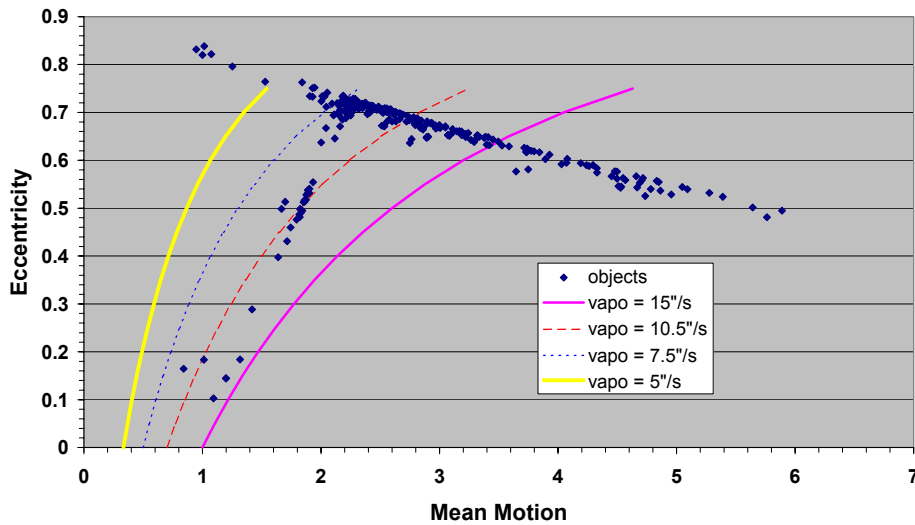


Figure 14: Eccentricity as a function of the mean motion for the objects in the catalogue.

4. CONCLUSIONS

Since 1999 ESA has been conducting several GEO and GTO survey campaigns using its 1-meter telescope on Tenerife. During the past year about 50% of the observation time was devoted to searches for objects in highly elliptical orbits, in particular in GTO orbits.

The results revealed a hitherto unknown but significant population of small-sized GEO debris in the size range from one meter to one decimeter. The magnitude distribution of this population is steeply increasing in the range from magnitude 15 to magnitude 19. The cutoff in number of objects fainter than about magnitude 19 – corresponding to an object size of about 15 centimeters – is entirely due to the sensitivity limit of the observation system. The real population of unknown small objects could therefore still increase beyond magnitude 19.

The several clusters of small objects sharing similar dynamical characteristics are the most remarkable result. The only reasonable explanation for the origin of these clusters are explosions.

A severe limitation of the surveys is given by the fact that circular orbits have to be inferred. Contaminations of the samples by objects on elliptical orbits were clearly seen, but are generally hard to identify. Real-time follow-up observations were performed to estimate elliptical orbits of a small sample of the discovered debris.

Reliable orbits could be estimated for a sample of 101 uncorrelated objects in elliptical orbits. Apart from objects in the GTO orbit region a considerable population of small-sized objects with a mean motion near one and eccentricities ranging from 0.05 to 0.5 was found. The nature and origin of this latter population is currently unknown.

5. REFERENCES

1. Schildknecht, T., U. Hugentobler, and A. Verdun, Algorithms for Ground Based Optical Detection of Space Debris, *Advances in Space Research*, Volume 16, Issue 11, p. 47-50, 1995.
2. Schildknecht, T., R. Musci, M. Ploner, G. Beutler, W. Flury, J. Kuusela, J. de Leon Cruz, and L. de Fatima Dominguez Palmero, *Optical Observations of Space Debris in GEO and in Highly-eccentric Orbits*, to be published in *Advances in Space Research*, 2003.
3. Schildknecht, T., Musci, R., Ploner, M., Preisig, S., de Leon Cruz, J., and Krag, H., *Optical Observation of Space Debris in the Geostationary Ring*, 3rd European Conference on Space Debris, 19 – 21 March 2001, ESOC, Darmstadt, Germany.